Inorganic Chemistry

Article

pubs.acs.org/IC

Ruthenium Carbon-Rich Complexes as Redox Switchable Metal Coupling Units

Emmanuel Di Piazza,[†] Areej Merhi,[†] Lucie Norel,*[,†] Sylvie Choua,*[,‡] Philippe Turek,[‡] and Stéphane Rigaut*[,†]

[†]UMR 6226 CNRS—Université de Rennes 1, Institut des Sciences Chimiques de Rennes, Campus de Beaulieu, F-35042, Rennes Cedex, France

[‡]UMR 7177 CNRS—Université de Strasbourg, Institut de Chimie, 1 rue Blaise Pascal, BP 296 R8, F-67008 Strasbourg Cedex, France

Supporting Information

ABSTRACT: With the help of EPR spectroscopy, we show that the diamagnetic $[Ru(dppe)_2(—C\equiv C—R)_2]$ system sets up a magnetic coupling between two organic radicals R, i.e., two nitronyl nitroxide or two verdazyl units, which is stronger than that of related platinum organometallic systems. Surprisingly, further oxidation of the ruthenium redox-active metal coupling unit (MCU), which introduces an additional spin unit on the carbon-rich part, leads to the switching off of this interaction. On the contrary, in simpler complexes bearing only one of the organic radical ligands $[C_6H_5—C\equiv C—Ru(dppe)_2—C\equiv C—R]$, one-electron oxidation of the transition metal unit generates an interaction between the two spin carriers of comparable magnitude to that observed in the above corresponding neutral systems.

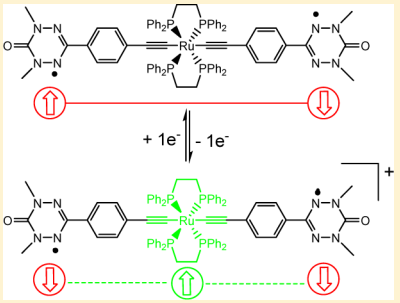

INTRODUCTION

Devices operating at the molecular level raise a great level of interest with the "bottom-up" approach expressed by Feynman in 1959.[1] In molecular-based switching devices, key physical properties such as optical, electric, or magnetic properties can be modulated with external stimuli.[2] To this end, group 8 metal acetylide complexes, displaying strong ligand-mediated electronic effects, are attractive redox-switchable candidates.[3,4] They allow modulation of different features as nonlinear optical,[5] luminescent,[6] magnetic,[7,8] or optical properties,[9,10] as well as conductivity.[11−16] Among them, ruthenium species with a trans ditopic structure are especially attractive owing to their exceptional ability to operate as a connector allowing electron flow to occur between different elements in multicomponent carbon-rich systems ("electronic communication"),[3a,8,17−22] and for the subsequent achievement of efficient molecular wires and junctions.[11,14,23,24]

As molecular magnetism is an attractive research area with respect to the promising new materials that might be prepared,[25] many efforts have also been invested in the elucidation of the role, sign, and magnitude of exchange coupling of unpaired electron in related [M]—C≡C—R—C≡C—[M] assemblies ("magnetic communication").[8,26] In contrast, nothing has been reported on the capacity of such metallic moieties to act as magnetic coupling units (MCU) between remote radicals, apart from a report on a platinum bis-ethynyl-phenyl-nitronyl-nitroxide complex displaying a weak coupling between the two radicals ($0.1 < |J| < 1$ cm^{-1}) through the nonredox active diamagnetic transition metal being known to be an inefficient mediator (Chart 1).[27] Therefore, it occurred to us that similar carbon-rich species including the redox active

Chart 1

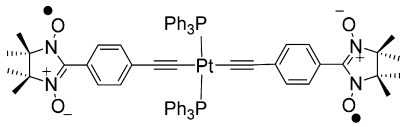

fragment $[Ru(dppe)_2(C\equiv CR)_2]$ (dppe = 1,2-bis-(diphenylphosphino)ethane), with orbitals delocalized on both the metal center and the acetylide ligands, should set up a more efficient magnetic coupling between the remote spin carriers. Another point of interest is related to the one-electron oxidation that creates a paramagnetic species with a unique electronic structure, since the spin density is largely delocalized on both the 4d ion and the carbon-rich ligands. Therefore, such properties should lead to a redox modulation of the coupling between the magnetic partners, a domain that has been less developed than the optical modulation,[7b,28−30] and that should be an advantage in the design of the new targeted materials compared with purely organic or inorganic molecules.

Hence, in this work, we have taken advantage of the $[Ru(dppe)_2(C\equiv CR)_2]$ system (i) to set up a magnetic coupling between two nitronyl nitroxide or two verdazyl units through this diamagnetic ruthenium unit, and (ii) to achieve not only the redox modulation of the exchange interaction between those radicals in such assemblies, but also to modify the magnetic behavior in simpler complexes bearing only one of these organic radical ligands (Scheme 1). These organic radicals have been selected because of their interest in the field of

Received: March 25, 2015
Published: June 12, 2015

DOI: 10.1021/acs.inorgchem.5b00667
Inorg. Chem. 2015, 54, 6347−6355

Scheme 1. Synthetic Pathways Yielding the Acetylide Complexes

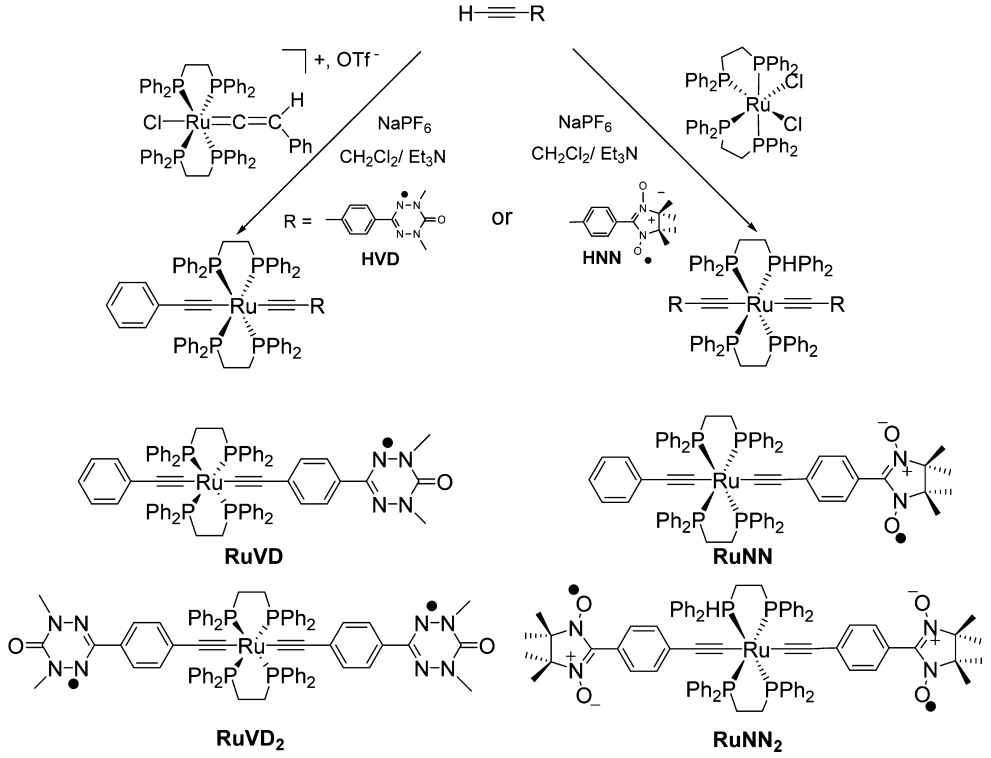

Scheme 2. Synthetic Pathways Yielding the HNV Ligand

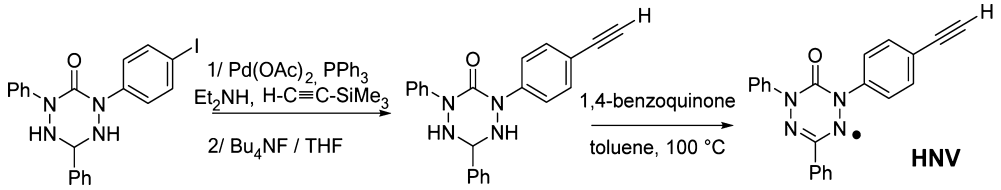

organic magnetism.[31−38] In particular, nitronyl nitroxides afforded the first purely organic magnet and they are widely studied to control intramolecular magnetic coupling. Furthermore, the ruthenium acetylide system displays a sufficiently low oxidation potential to avoid the radical oxidations.[39] Two types of connection of the verdazyl unit with the metal unit were attempted, via a carbon atom or a nitrogen atom (Scheme 2), as stronger magnetic coupling was expected in the latter case.[37c,40] With all complexes, the strengths of the intramolecular interactions were properly assessed in the isolated state (dilute solution) with EPR spectroscopy.

RESULTS AND DISCUSSION

Complex Synthesis. The syntheses of the targeted complexes were attempted following the well-established procedure to achieve unsymmetrical and symmetrical bis(alkynyl)ruthenium complexes (Scheme 1).[41] Therefore, the ruthenium vinylidene bearing a phenyl group was reacted with 1 equivalent (equiv) of the appropriate verdazyl (HVD)[42] or nitronyl nitroxide (HNN)[33] alkyne in the presence of a base and a chloride abstracting agent to yield RuVD and RuNN. The two complexes were purified by column chromatography on alumina gel under an argon atmosphere and obtained as green powders with moderate yields (53 and 41%, respectively). For the symmetrical $RuVD_2$ and $RuNN_2$ complexes, *cis*-$[RuCl_2(dppe)_2]$ was reacted under similar conditions with 2 equiv of the appropriate alkyne to afford the targeted complexes with isolated yields of 51 and 46%, respectively. As characteristic features, we observed the expected $\upsilon_{C\equiv C}$ vibration stretch for the acetylide complexes at 2057 and 2054 cm^{-1} for RuVD and $RuVD_2$ in the Fourier transform infrared (FTIR) spectra, along with characteristic C═O stretching from the verdazyl part at 1685 and 1689 cm^{-1} for RuVD and $RuVD_2$, respectively. The acetylide vibration stretches were detected at 2052 and 2050 cm^{-1} for RuNN and $RuNN_2$, along with the υ_{N-O} vibration at 1357 and 1360 cm^{-1}, respectively. The purity of the compounds was further assessed with the help of chromatography, high resolution mass spectrometry (HR-MS), cyclic voltammetry, and EPR measurement (vide infra). However, even when it was stored at −15 °C, the $RuVD_2$ complex showed progressive degradation with time.

We further obtained the new related ethynyl functionalized "N-linked" verdazyl radical 1-aryl-3,5-diphenyl-6-oxoverdazyl radical HNV from the 1-(4-iodophenyl)-3,5-diphenyl-6-oxo-1,2,4,5-tetrazane via copper free Sonogashira coupling with trimethylsilylacetylene, followed by deprotection and oxidation with benzoquinone (Scheme 2). Unfortunately, this compound appeared to be unstable for further achievement of the ruthenium complexes.

Electrochemical Studies. Cyclic voltammetry (CV) was used to study the electrochemical behavior of all complexes

DOI: 10.1021/acs.inorgchem.5b00667
Inorg. Chem. 2015, 54, 6347−6355

Table 1. Electrochemical and Optical Data

	electrochemistry,[a] $E°$/V				
	$E°(-/0)$	$E°(0/+)$	$E°(+/n+)$	UV−vis,[b] λ_{max}/nm (ε/mol^{-1}·L·cm^{-1})	UV−vis[c] of oxidized species, λ_{max}/nm (ε/mol^{-1}·L·cm^{-1})
RuVD	−1.42[d]	−0.01	0.30[e] (n = 2)	244 (50 000), 321 (15 800), 379 (27 000), 560 (300)	622 (1100), 1161 (5265)
RuVD2	−1.25[d]	0.02	0.31[e] (n = 3)	267 (72 000), 385 (60 000), 572 (1100)	526 (nd), 1190 (nd)
HVD	−1.34[df]	0.33[f]		277 (43 000), 425 (1560), 485 (470)	–
RuNN		0.02	0.41 (n = 2)	230 (50 000), 314 (sh,16 200), 372 (18 100), 658 (450)	230 (49 900), 314 (16 100), 1160 (2200)
$RuNN_2$		0.06	0.41 (n = 3)	234 (44 900), 372 (24 850), 395 (sh, 22 600), 598 (350)	218 (84 500), 374 (31 300), 1206 (3900)
HNN		0.42		294 (16 000), 376 (9600), 598 (300)	–

[a]Sample 1 mM, Bu_4NPF_6 (0.2 M) in CH_2Cl_2, v = 100 mV·s^{-1} (potentials are reported in V vs $FeCp_2/FeCp_2^+$ as an internal standard), reversible oxidation processes, $\Delta E_p \approx 60$ mV. [b]In CH_2Cl_2. [c]In 0.2 M NBu_4PF_6/1,2-$C_2H_4Cl_2$. [d]$\Delta E_p \approx 200$ mV. [e]$\Delta E_p \approx 80$ mV. [f]See ref 42.

(CH_2Cl_2, 0.2 M Bu_4NPF_6). Characteristic data are reported in Table 1, where the values for the organic radicals are also presented for comparison, and typical CV traces are presented in Figure 1. In addition to a high potential chemically

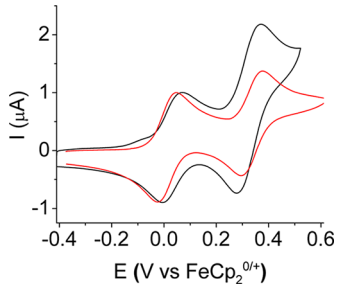

Figure 1. CV traces of RuVD (red line) and $RuVD_2$ (black line) in CH_2Cl_2 (0.2 M Bu_4NPF_6, v = 100 mV·s^{-1}).

irreversible event (see Supporting Information), three processes are observed for RuVD and $RuVD_2$. The electrochemically irreversible reduction process at negative potential is also observed for the parent verdazyl ligand (Table 1) and is characteristic of the reduction of the oxoverdazyl moiety.[43] The first and second oxidation waves are respectively ascribed to a ruthenium bis-acetylide centered process and to a verdazyl centered oxidation by comparison with related ruthenium bis-acetylides and with HVD oxidation potential. More specifically, (i) the first oxidation event, close to that of ferrocene, is a fast reversible monoelectronic process with a potential value characteristic of the organometallic core bearing one or two weak electron-withdrawing groups[44] as the oxoverdazyl rings which have been shown to be as withdrawing as nitrogen heterocycles,[43] and (ii) the verdazyl centered oxidation in RuVD and $RuVD_2$ complexes has a very similar oxidation potential to that of the parent ligand. The apparent 1:2 ratio between the current intensity of the first oxidation wave and that of the second one in $RuVD_2$ nicely confirms the efficient functionalization of the ruthenium core by two verdazyl ligands. In addition, the low ΔE_p value for this later process shows that both verdazyl substituents are almost concomitantly oxidized, indicating that these oxidation processes are rather localized on independent verdazyl rings in the fundamental state. Overall, the nitronyl nitroxide complexes RuNN and $RuNN_2$ display similar behaviors, i.e., with a first reversible process ascribed to the carbon-rich moiety and a second reversible oxidation centered on the organic radical(s) and comparable with that of the free organic ligand HNN. As expected, the $RuNN_2$ diradical also displays two overlapping one-electron-oxidation processes due to the presence of two nitronyl nitroxide ligands.

Optical Properties. The electronic properties of the four complexes were investigated in the neutral state and in their first oxidized state during electrochemical oxidation (Table 1, Figure 2). The neutral complexes all display a band

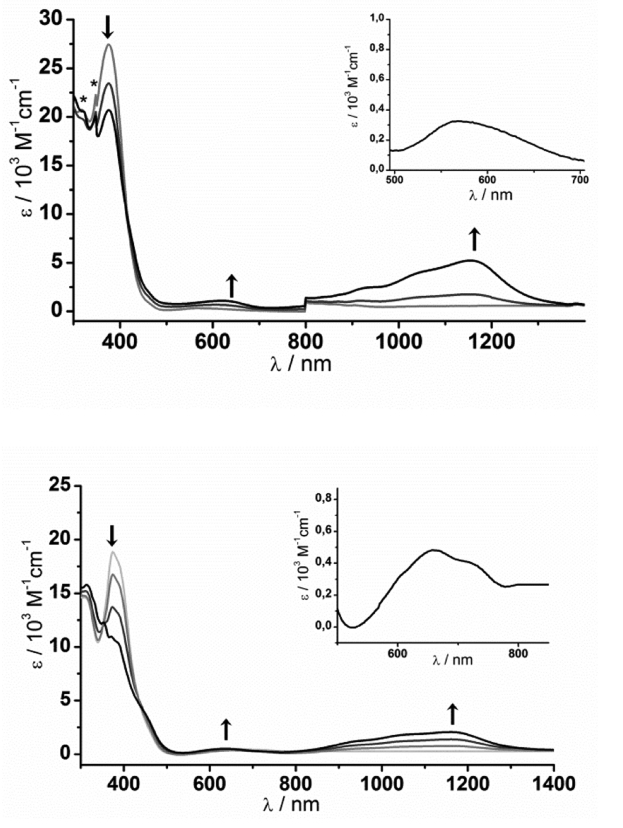

Figure 2. Absorption spectra and spectroscopic changes for (top) RuVD and (bottom) RuNN in the UV/vis/NIR range during their first oxidation in 0.2 M NBu_4PF_6/1,2-$C_2H_4Cl_2$. Insets magnify the low intensity bands related to the radical units of the neutral species.

characteristic of ruthenium acetylide systems at $\lambda_{max} \approx 380$ nm, usually described as multiconfigurational metal-to-ligand charge transfer (MLCT) excitations corresponding to transitions from Ru($d\pi$)/alkynyl-based orbitals to metal/ligand antibonding orbitals combined with intraligand (IL) $\pi \rightarrow \pi^*$ character.[18,44] Their green color in dichloromethane solution is related to their weak absorption band in the visible range of the

DOI: 10.1021/acs.inorgchem.5b00667
Inorg. Chem. 2015, 54, 6347−6355

spectra around 550−650 nm due to the verdazyl or nitronyl nitroxide radical parts. We further studied the modification of these electronic spectra during electrochemical oxidation in an optically transparent thin-layer electrochemical (OTTLE) cell. The oxidation potential of the device was set between the first and second oxidation potentials of each complex in order to perform oxidation of the organometallic core only. Indeed, further oxidation occurred to be irreversible on the time scale of the experiments. Thus, upon the first oxidation, the most striking features are (i) the decrease of the "MLCT" band, and (ii) the concomitant appearance of a new low energy transition in the near-IR (NIR) range with a maximum at $\lambda_{max} \approx 1160-1200$ nm and displaying shoulders at higher energy. A closer inspection of the energy plot of these NIR bands reveals that the shoulders result from the overlap of several transitions spaced by ca. 1000 cm^{-1} (see Supporting Information, Figure S6, on the example of $RuVD^{+}$). They are consistent with observations reported by Low and co-workers[45] on related carbon-rich ruthenium acetylides, who assigned such envelopes to the presence of different thermally accessible conformational structures due to relative orientations of the metal fragment and arylethynyl moieties. Such bands were also recently observed upon oxidation of related ruthenium metal acetylides bearing a bipyridine unit complexed to a lanthanide ion.[6] They are probably due to transitions from the highest occupied molecular orbital (HOMO) − n to the singly occupied molecular orbital (SOMO) resulting from the depopulation of the HOMO $d\pi/\pi$ orbital. While the bands involve some charge transfer between the metal groups and the carbon-rich ligand, they certainly also exhibit a strong $\pi \rightarrow \pi^*$ (IL) character. In addition, in the case of RuVD and $RuVD_2$, the low extinction band at 560 nm is also red-shifted (by 70 nm) and slightly enhanced during oxidation, whereas in the case of RuNN and $RuNN_2$, it remains unchanged. While the other compounds show a reversibility of 90% or higher on the spectroelectrochemical (SEC) experiment time scale, the $RuVD_2$ complex displays a poorer reversibility of ca. 50%, consistent with the above-mentioned instability of the complex and also with the EPR observation (vide infra). In parallel, IR spectroelectrochemical experiments were conducted with RuNN and $RuNN_2$ (Supporting Information, Figure S7); both complexes display an expected shift of the $\upsilon_{C\equiv C}$ vibration stretch from 2052 and 2050 cm^{-1} to 1903 and 1897 cm^{-1}, respectively, upon one-electron removal. This results from the bond weakening of the acetylide linkages upon one-electron removal confirming a large involvement of the central bis(ethynyl) ruthenium moiety in the first oxidation process.[41b,45]

EPR Measurements. The magnetic properties of the different compounds have been investigated by EPR performed at X-band ($\nu_0 \sim 9.5$ GHz). The EPR spectrum of RuNN single radical in solution (Figure 3) shows the expected five-line pattern for a nitronyl nitroxide radical.[32,33] The experimental spectrum was best simulated with a nitrogen hyperfine coupling constant (hfcc) of 8.5 G, whereas the hfcc coupling with ^{101}Ru and ^{99}Ru nuclei (I = 5/2, natural abundance 17 and 12%, respectively) was not observed. Regarding the lack of the observation of the so-called forbidden lines assigned to transitions at $H_0/2$ ($\Delta M_S = \pm 2$) for the triplet spin state and at $H_0/3$ ($\Delta M_S = \pm 3$) for the quartet spin state, it is worth noticing that the observation of a $H_0/3$ line has been scarcely reported within pure organic triradicals. For instance, neither the $H_0/2$ transition nor the $H_0/3$ one was observed for some

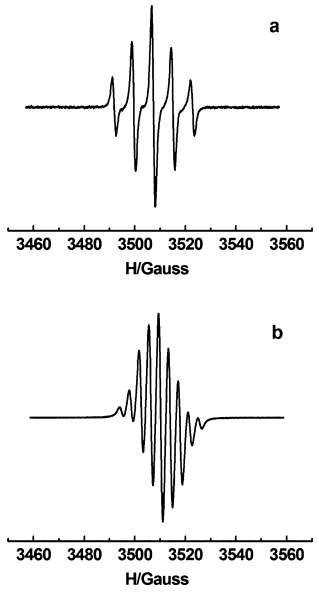

Figure 3. X-band EPR experimental spectra (a) of RuNN and (b) $RuNN_2$ in CH_2Cl_2 diluted solution at room temperature.

organic triradicals based on nitroxide.[59] The observed 13-line pattern of RuVD (Figure 4) is due to the hfcc coupling of two sets of different nitrogen nuclei ($a(^{14}N_1)$ = 6.5 G; $a(^{14}N_2)$ = 5.3 G) and six ^1H nuclei ($a(^1H)$ = 5.3 G).[46]

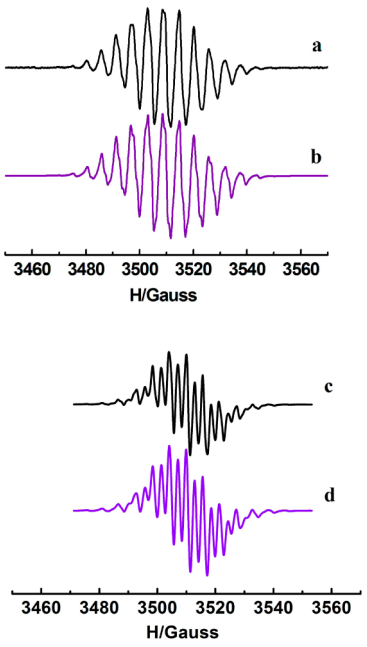

Figure 4. X-band EPR spectra in CH_2Cl_2 diluted solution at room temperature: (a) experimental spectrum of RuVD; (b) simulated spectrum; (c) experimental spectrum of $RuVD_2$; (d) simulated spectrum.

The EPR spectrum of the diradical derivative $RuNN_2$ in solution perfectly fits with a two-spin species with $a(^{14}N_{RuNN})/2 = a(^{14}N_{RuNN_2})$.[36] In the frame of EPR spectroscopy, this situation corresponds to the strong exchange limit and means that the exchange coupling is much higher than the hyperfine coupling. Due to its instability (vide supra), attempts to observe the pure $RuVD_2$ compound in solution were unsuccessful. The

DOI: 10.1021/acs.inorgchem.5b00667
Inorg. Chem. 2015, 54, 6347−6355

spectrum of $RuVD_2$ corresponds in fact to a mixture of two species.[37c] A good simulation was obtained by assuming an admixture of 15% of one system bearing only one verdazyl unit (issued from evolution) and 85% of $RuVD_2$ ($a(^{14}N_1)$ = 3.1 G; $a(^{14}N_2)$ = 2.6 G ; $a(^{1}H)$ = 2.8 G).[47,48]

The frozen solution EPR spectrum of $RuNN_2$ recorded at 4 K exhibits only one intense symmetrical line (ΔB_{PP} = 11 G) centered on g = 2.0 without any fine structure characteristic of the triplet state. In the case of the $RuVD_2$ compound, a similar spectrum (ΔB_{PP} = 21 G) was observed and the forbidden ΔM_s = ±2 transition was detected at half-field. This definitely signs the biradical nature of the compound (see Supporting Information, Figure S8).

The temperature dependence of the EPR signal intensities points to weak antiferromagnetic coupling (Figure 5). Note

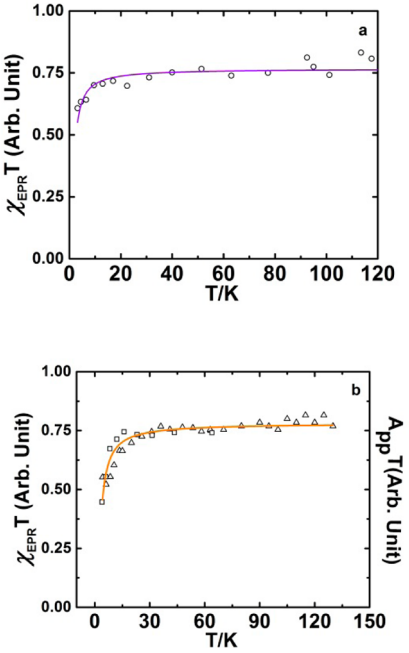

Figure 5. Temperature dependence of the EPR susceptibility (χT product) in CH_2Cl_2 frozen solution: (a) ○, integrated intensity $\chi_{EPR}T$ for ΔM_s = ±1 line for $RuNN_2$, (b) △, integrated intensity $\chi_{EPR}T$ for ΔM_s = ±1 line for $RuVD_2$; □, peak-to-peak amplitude for ΔM_s = ±2 for $RuVD_2$. The continuous line represents the fit for a two-spin model.

that the EPR susceptibility is assessed as usual with the integrated intensity for the ΔM_s = ±1 line with a high signal-to-noise ratio, while it is given by the peak-to-peak amplitude for the weak ΔM_s = ±2 signal.[32a] This is correct as far as the line shape does not vary. This procedure allows discarding possible deviations due to ill-defined baseline or microwave power saturation effects at low temperature. The experimental data were fitted by a Bleaney–Bowers expression[49] for an isolated two-spin model ($H = -JS_1S_2$) with an additional contribution of a Curie law for $RuVD_2$ to account for the presence of the single radical. A singlet–triplet splitting of J = −2.1 cm^{-1} and J = −4.2 cm^{-1} is assessed for $RuNN_2$ and $RuVD_2$, respectively. Note that the accuracy on the J value is given by the fitting process (~10%). For $RuNN_2$ singlet and triplet spin states can be considered as quasi-degenerate, whereas for $RuVD_2$ the singlet–triplet (ST) gap is more important. It is worth noting that the study of the exchange interaction through a diamagnetic metal core[27,50] is less documented as compared to π spacers.[32–34,36] The present $RuVD_2$ and $RuNN_2$ compounds offer a quite rare example of a diradical species with an organometallic ruthenium core as a spacer (Table 2).

Table 2. Comparison between Organic and Organometallic Magnetic Coupling Units (MCU)

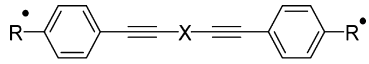

	X	R•	J^a/cm^{-1}
Ph	1,4-(2,5-bis(dodecanoxy) phenyl)	imino nitroxide	−2.2[33]
Pt	$Pt(PPh_3)_2$	nitronyl nitroxide	−1 < J < −0.1[27]
$RuVD_2$	$Ru(dppe)_2$	verdazyl	−4.2 [this work]
$RuNN_2$	$Ru(dppe)_2$	nitronyl nitroxide	−2.1 [this work]

$^aH = -JS_1S_2$.

They show exchange interactions of the same nature (antiferromagnetic, AF) but of smaller strength as compared with the ruthenocene core (−38 cm^{-1}), and probably established through a similar spin polarization mechanism.[51] However, the distance between the remote radical termini in our systems is much larger so that, with comparable (imino or nitronyl nitroxide) diradicals, 1,4-(2,5-bis(dodecanoxy)phenyl) and $Pt(PPh_3)_2$ offer a better point of comparison with the $Ru(dppe)_2$ core.

When comparing Ph and Pt spacers, the platinum based organometallic moiety within the organic spacer leads to a smaller singlet–triplet (ST) exchange splitting. Moving to ruthenium yields an ST gap similar to that for an aromatic fragment as in Ph. Therefore, the d orbitals of the diamagnetic transition metal are probably involved in a superexchange-like pathway. The apparent better efficiency of a ruthenium center compared to a platinum one in promoting electronic coupling with the alkynyl ligand may express the expected better π–d hybridization through orbital overlap.

The other interest of the studied compounds is related to the possibility of generating a third magnetic actor as a paramagnetic metallic center on the metal site. As the first oxidation waves of mono and bis compounds were attributed to a ruthenium bis(acetylide) centered process, the magnetic coupling has been subsequently studied after chemical oxidation.[52] Singly oxidized species were generated by addition of $KAuCl_4$[53] in CH_2Cl_2 to afford the corresponding monooxidized $RuNN^+$, $RuNN_2^+$ and $RuVD^+$, $RuVD_2^+$ cations at room temperature. The peculiar features due to the presence of triplet spin state or of quartet spin state, being expected after oxidation respectively for the monoradical or for the diradical derivatives, were not systematically observed. The compounds $RuVD^+$ and $RuVD_2^+$ show similar EPR spectra in frozen solution with a single line centered at g = 2 (ΔB_{PP} = 21–22 G). The occurrence of a biradical is signed by a half-field transition ($g \sim 4$) for $RuVD^+$ (see Supporting Information, Figure S9). A broad single line is observed at 4 K for $RuNN^+$ (ΔB_{PP} = 25 G) and $RuNN_2^+$ (ΔB_{PP} = 21 G). The line width decreases as the temperature increases and some structure is observed beneath, which becomes more visible. The observed spectra are similar to that of phenyl-monoNN (see Supporting Information, Figures S10 and S11).[54] The temperature dependence of the EPR susceptibility χ_{EPR} corresponding to the integrated EPR

DOI: 10.1021/acs.inorgchem.5b00667
Inorg. Chem. 2015, 54, 6347–6355

signal has been measured for all of the generated cations (Figure 6). Experimental data for the monooxidized species can

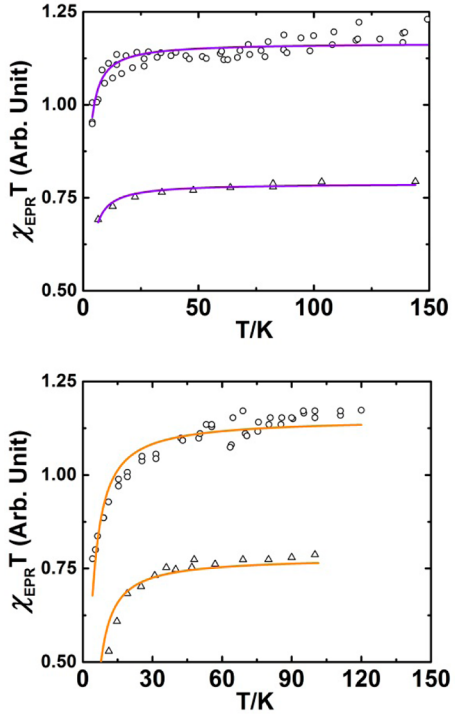

Figure 6. Temperature dependence of the EPR susceptibility (χT product) in CH_2Cl_2 frozen solution: (top) ○, $RuNN_2^+$ ($\Delta M_s = \pm 1$ line); △, $RuNN^+$ ($\Delta M_s = \pm 1$ line). The continuous line represents a fit for a three-spin model. (bottom) ○, integrated intensity $\chi_{EPR}T$ for $\Delta M_s = \pm 1$ line for $RuVD_2^+$. The continuous line represents a fit for a three-spin model. △, peak-to-peak amplitude for $\Delta M_s = \pm 2$ line for oxidized $RuVD^+$.

be reproduced by a singlet−triplet equilibrium, for both $RuVD^+$ and $RuNN^+$. The magnetic behavior of the oxidized biradical species has been simulated upon assuming the coexistence of neutral and oxidized species, i.e., the addition of a linear three-spin model with two identical J exchange couplings[55] and a two-spin model.

$$\chi T = C\left\{2x\left(\frac{3}{3 + \exp(-J_{ST}/k_BT)}\right) + 0.75(1 - x)\left[\frac{10 + \exp(-3J_{3S}/k_BT) + \exp(-J_{3S}/k_BT)}{2 + \exp(-3J_{3S}/k_BT) + \exp(-J_{3S}/k_BT)}\right]\right\}$$

In this expression, J_{3S} represents the doublet−quartet splitting and J_{ST} is the singlet−triplet splitting. The Curie constant C is that for an $S = 1/2$ spin, and x is the amount of two-spin species. The obtained values are reported in Table 3. To assess the level of confidence of the J values the fit parameters have been obtained, while, e.g., doubling the x values. The obtained J values for the three-spin systems are thus affected by ca. 20% at most.

Magnetic studies performed on $RuVD_2$ and $RuNN_2$ biradicals before oxidation gave us an assessment of the J value between two organic spin carriers through a diamagnetic Ru(II) center. We could now compare them with $RuVD^+$ and $RuNN^+$ after oxidation of the Ru(II) carbon-rich center, keeping in mind that the magnetic coupling in these derivatives

Table 3. EPR Parameters (hfcc's) and Exchange Coupling Data for Complexes in CH_2Cl_2 Dilute Solution

complex	g_{iso}	a_N^{iso}/G	a_H^{iso}/G	J/cm^{-1}
RuNN	2.004	8.5	–	–
$RuNN_2$	2.005	3.8	–	−2.1
RuVD	1.990	6.5; 5.3	5.3	–
$RuVD_2$	1.991	3.1; 2.6	2.8	−4.2
$RuNN^+$	~2.0[a]	–	–	−2.2
$RuNN_2^+$	~2.0[a]	–	–	−0.7[b]
$RuVD^+$	~2.0[a]	–	–	−4.2
$RuVD_2^+$	~2.0[a]	–	–	−1.8[b]

[a]Value in frozen solution at 4 K. [b]The amount of two-spin species, x = 0 for $RuNN_2^+$ and x = 0.15 for $RuVD_2^+$ as concluded from EPR in solution at RT.

sets up between an organic radical and a metal at a shorter interspin distance than in $RuVD_2$ and $RuNN_2$. First, the ST gaps of $RuVD^+$ and $RuNN^+$ are similar to those of $RuVD_2$ and $RuNN_2$, respectively. This is quite surprising, since it may be considered that through bond spin exchange is mediated via diamagnetic metal orbitals within $RuVD_2$, while it is a direct metal spin-radical spin coupling within $RuVD^+$. It is therefore amazing that the magnetic switch is counterproductive for the improvement of magnetic exchange, as it is observed that the presence of a third spin carrier causes a decrease of the magnetic coupling within $RuVD_2^+$, while switching it off in $RuNN_2^+$. In situ electrolysis of $RuNN_2$ compound at room temperature was performed to confirm the results obtained after chemical oxidation. Applying a potential matching the first oxidation potential (vs Ag as reference electrode) leads to an admixture of mono- and biradical components after a few minutes of electrolysis (Supporting Information, Figure S12). This strengthens the observation that the presence of a third spin center on Ru switches off the magnetic coupling exchange between the two remote side radical spin carriers. To rule out a parallel decomposition of the compound, it was observed that applying a negative potential could regenerate the EPR spectrum of the biradical.

Concluding Remarks. In this work, we have shown with the help of EPR spectroscopy that in simple complexes bearing one nitronyl nitroxide or verdazyl radical ligand [C_6H_5—C≡C—Ru(dppe)$_2$—C≡C—R], one-electron oxidation of the transition metal carbon-rich unit generates an antiferromagnetic spin alignment between the two spin carriers of ca. 2 and 4 cm^{-1} for nitronyl nitroxide and verdazyl radicals, respectively. Interestingly, the diamagnetic [Ru(dppe)$_2$(—C≡C—R)$_2$] system is able to set up a similar magnetic coupling between two remote radical units, i.e., nitronyl nitroxide (−2 cm^{-1}) or two verdazyl radicals (−4 cm^{-1}), in a more efficient way than the related platinum organometallic system (see Table 2). Unexpectedly, while introducing an additional spin unit on the metal MCU, oxidation leads to the decrease or the switching off of these interactions (~ −1 and ~ −2 cm^{-1}, respectively). A Hubbard model could be considered to explain qualitatively the mechanism taking place in oxidized compounds. The spin delocalization and the through bond magnetic interaction may involve a double occupancy of the Ru site. The on-site Coulomb repulsion (U) could then oppose the setup of magnetic interaction and/or electron delocalization (t), thus lowering the magnetic exchange interaction according to the t^2/U dependence of the exchange interaction in such a localized Heisenberg scheme.[56] Alternatively, another explanation could

DOI: 10.1021/acs.inorgchem.5b00667
Inorg. Chem. 2015, 54, 6347−6355

rely on the fact that the oxidation processes shift the energy level of the ruthenium core, preventing the magnetic coupling via an efficient polarization mechanism, a point currently under investigation with the help of theoretical calculations.

EXPERIMENTAL SECTION

General Comments. The reactions were carried out under an inert atmosphere using Schlenk techniques. Solvents were dried and distilled under argon using standard procedures. HR-MS spectra were recorded on a Bruker MicrO-Tof-Q 2 spectrometer. The ruthenium complexes *trans*-[Cl(dppe)$_2$Ru=C=CHPh][OTf],[57] *cis*-(dppe)$_2$RuCl$_2$,[58] radical HVD,[42] and HNN[33] have been obtained as previously reported.

Electrochemical studies were carried out under argon using an Eco Chemie Autolab PGSTAT 30 potentiostat (CH_2Cl_2, 0.2 M Bu_4NPF_6), the working electrode was a Pt disk, and ferrocene was the internal reference. UV−vis−NIR spectroelectrochemistry (SEC) experiments were performed at 20 °C, under argon, with a homemade optically transparent thin-layer electrochemical (OTTLE) cell, path length = 1 mm, using a Varian CARY 5000 spectrometer and an EG&G PAR Model 362 potentiostat. A Pt mesh was used as the working electrode, a Pt wire was used as the counter electrode, and an Ag wire was used as a pseudoreference electrode. The electrodes were arranged in the cell such that the Pt mesh was in the optical path of the quartz cell. The anhydrous freeze−pump−thaw degassed sample-electrolyte solution (0.2 M *n*-Bu_4NPF_6) was cannula-transferred under argon into the cell previously thoroughly deoxygenated. IR experiments were performed under similar conditions using a modified cell with KBr windows and a Bruker IFS28 spectrometer.

EPR spectra were recorded on a Bruker EMX spectrometer operating at X-band (9.4 GHz) with a standard rectangular cavity (TE 102). An ESR900 cryostat (Oxford Instruments) was used for the low temperature measurements. Sample solutions in quartz tubes were degassed by three freeze-and-thaw cycles.

The in situ electrolysis under argon atmosphere and at controlled potential with a three electrode configuration (platinum wire working electrode, platinum wire auxiliary electrode, and Ag wire as pseudoreference electrode) was performed in a homemade cell with Bu_4NPF_6 (0.1 M) as a supporting electrolyte.

***trans*-[Ru(dppe)$_2$(—C≡C—Ph)(—C≡C—*p*-C$_6$H$_4$—C$_{14}$H$_{10}$N$_4$O•)] (RuVD).** *trans*-[Ru=C=CHPh(Cl)(dppe)$_2$][OTf] (261 mg, 0.22 mmol), $NaPF_6$ (74 mg, 0.44 mmol, 2 equiv), and 1,5-dimethyl-3-(*p*-ethynylphenyl)-6-oxoverdazyl (HVD) (55 mg, 0.24 mmol, 1.1 equiv) were dissolved in 15 mL of CH_2Cl_2. Triethylamine was then added with 10 mL of dichloromethane. The red solution progressively changed color to dark green upon stirring at room temperature for 2 h. It was then evaporated under vacuum. The product was filtered on a plug of alumina using CH_2Cl_2 as eluent. The dark green fraction was collected and concentrated under vacuum to yield approximately 5 mL of solution. Pentane was added to induce the precipitation of a green solid. The red filtrate contained mostly excess radical. After filtration, a green powder was obtained (143 mg, 53%). IR (KBr, cm^{-1}): 3050, 2920 (υ_{C-H}), 2057 ($\upsilon_{C\equiv C}$), 1685 ($\upsilon_{C=O}$). MS-ESI (*m*/*z*): [M + Na]$^+$ = 1248.2907 (calculated 1248.28881).

***trans*-[Ru(dppe)$_2$(—C≡C—*p*-C$_6$H$_4$—C$_{14}$H$_{10}$N$_4$O•)$_2$] (RuVD2).** $NaPF_6$ (160 mg, 0.95 mmol), *cis*-$RuCl_2$(dppe)$_2$ (284 mg, 0.29 mmol), and 1,5-dimethyl-3-(*p*-ethynylphenyl)-6-oxoverdazyl (HVD) (160 mg, 0.70 mmol) were dissolved in 60 mL of dichloromethane. Triethylamine (0.81 mL) was added. The red solution progressively changed color to dark green upon stirring at room temperature for one night. The mixture was concentrated under vacuum to yield a green powder which was purified by chromatography (alumina/dichloromethane). The dark green fraction was collected and concentrated under vacuum to yield approximately 5 mL of solution. Pentane was added to induce the precipitation of a green solid (198 mg, 51%). The red filtrate contained mostly excess radical. IR (KBr, cm^{-1}): 3053, 2925 (υ_{C-H}), 2054 ($\upsilon_{C\equiv C}$), 1689 ($\upsilon_{C=O}$). MS-ESI (*m*/*z*): [M + Na]$^+$ = 1373.3372 (calculated 1373.33514).

***trans*-[Ru(dppe)$_2$(—C≡C—Ph)(—C≡C—*p*-C$_6$H$_4$—C$_7$H$_{12}$N$_2$O$_2$•)] (RuNN).** In a Schlenk tube, *trans*-[ClRu(dppe)$_2$=C=CH—Ph][OTf] (150 mg, 0.127 mmol), $NaPF_6$ (42.5 mg, 0.253 mmol), and H—C≡C—*p*-C$_6$H$_4$—C$_7$H$_{12}$N$_2$O$_2$• (HNN) (42.5 mg, 0.165 mmol) were dried under vacuum for 30 min. Then, degassed dichloromethane (25 mL) was transferred into the Schlenk tube. Triethylamine (1 mL) was then added drop by drop. The mixture reacted at room temperature for 2 h, and then the solution was filtered and taken to dryness under vacuum. The residue was chromatographed (alumina, CH_2Cl_2) under argon to obtain a green powder (65.2 mg, 41%). IR (KBr, cm^{-1}): 2052 ($\upsilon_{C\equiv C}$), 1357 (υ_{N-O}). FAB$^+$-MS (*m*/*z*) [M]$^+$ = 1255.3368 (calculated 1255.33476).

***trans*-[Ru(dppe)$_2$(—C≡C—*p*-C$_6$H$_4$—C$_7$H$_{12}$N$_2$O$_2$•)$_2$] (RuNN2).** In a Schlenk tube, *cis*-$RuCl_2$(dppe)$_2$, (75 mg, 0.078 mmol), $NaPF_6$ (65.2 mg, 0.388 mmol), and H—C≡C—*p*-C$_6$H$_4$—C$_7$H$_{12}$N$_2$O$_2$• (HNN) (50 mg, 0.194 mmol) were dried under vacuum for 30 min. Degassed dichloromethane (30 mL) was added with a syringe afterward. Then, triethylamine (1 mL) was added drop by drop. The mixture reacted at room temperature for 4 h, and then the solution was filtered and taken to dryness under vacuum. The residue was chromatographed (alumina, CH_2Cl_2) under argon to obtain a green powder (50 mg, 46%). IR (KBr, cm^{-1}): 2050 ($\upsilon_{C\equiv C}$), 1360 (υ_{N-O}). HR-MS (ESI) (*m*/*z*) [M]$^+$ = 1410.4195 (calculated 1410.41681).

ASSOCIATED CONTENT

Supporting Information

Synthetic procedures as well as CVs, SEC spectra, and EPR spectra. The Supporting Information is available free of charge on the ACS Publications website at DOI: 10.1021/acs.inorgchem.5b00667.

AUTHOR INFORMATION

Corresponding Authors

*E-mail: stephane.rigaut@univ-rennes1.fr (S.R.).
*E-mail: lucie.norel@univ-renes1.fr (L.N.).
*E-mail: sylvie.choua@unistra.fr (S.C.).

Notes

The authors declare no competing financial interest.

ACKNOWLEDGMENTS

We thank the Université de Rennes 1, the CNRS, the ANR (Photomagcom—ANR-12-BS07-0010-01), the Région Bretagne (Ph.D. grant for E.D.P.) for support, and the POMAM group in Strasbourg.

REFERENCES

(1) Richard Feynman's original lecture, "Plenty of Room at the Bottom": www.its.caltech.edu/~feynman.

(2) *Molecular Switches*; Feringa, B. L., Browne, R. W., Eds.; Wiley-VCH: Weinheim, 2011. *Spin-Crossover Materials: Properties and Applications*; Halcrow, M. A., Ed.; Wiley-VCH: Weinheim, 2013. Ohkoshi, S.-I.; Tokoro, H. *Acc. Chem. Res.* **2012**, *45*, 1749. Hicks, R. G. *Nat. Chem.* **2011**, *3*, 189.

(3) (a) Costuas, K.; Rigaut, S. *Dalton Trans.* **2011**, *40*, 5643. Aguirre-Etchevery, P.; O'Hare, D. *Chem. Rev.* **2010**, *110*, 4839. Low, P. J.; Brown, N. J. *J. Clust. Sci.* **2010**, *21*, 235. Záliš, S.; Winter, R. F.; Kaim, W. *Coord. Chem. Rev.* **2010**, *254*, 1383. Ren, T. *Organometallics* **2005**, *24*, 4854. Akita, M.; Koike, T. *Dalton Trans.* **2008**, 3523. Venkatessan, K.; Blacque, O.; Berke, H. *Dalton Trans.* **2007**, 1091. Bruce, M. I.; Low, P. J. *Adv. Organomet. Chem.* **2004**, *50*, 179. Szafert, S.; Gladysz, J. A. *Chem. Rev.* **2003**, *103*, 4175. Aguirre-Etchevery, P.; O'Hare, D. *Chem. Rev.* **2010**, *110*, 4839. Low, P. J. *Coord. Chem. Rev.* **2013**, *257*, 1507.

(4) Rigaut, S. *Dalton Trans.* **2013**, *42*, 15859.

(5) Samoc, M.; Gauthier, N.; Cifuentes, M. P.; Paul, F.; Lapinte, C.; Humphrey, M. G. *Angew. Chem., Int. Ed.* **2006**, *45*, 7376. Green, K. A.;

DOI: 10.1021/acs.inorgchem.5b00667
Inorg. Chem. 2015, 54, 6347−6355

Cifuentes, M. P.; Samoc, M.; Humphrey, M. G. *Coord. Chem. Rev.* **2011**, *255*, 2530.
(6) Di Piazza, E.; Norel, L.; Costuas, K.; Bourdolle, A.; Maury, O.; Rigaut, S. *J. Am. Chem. Soc.* **2011**, *133*, 6174. Norel, L.; Di Piazza, E.; Feng, M. A.; Vacher, A.; He, X.; Roisnel, T.; Maury, O.; Rigaut, S. *Organometallics* **2014**, *33*, 4824. Wong, K. M.-C.; Lam, S. C.-F.; Ko, C.-C.; Zhu, N.; Yam, V. W.-W.; Roué, S.; Lapinte, C.; Fathallah, S.; Costuas, K.; Kahlal, S.; Halet, J.-F. *Inorg. Chem.* **2003**, *42*, 7086.
(7) Norel, L.; Bernot, K.; Feng, M.; Roisnel, T.; Caneschi, A.; Sessoli, R.; Rigaut, S. *Chem. Commun.* **2012**, *48*, 3948. (b) Norel, L.; Min, F.; Bernot, K.; Roisnel, T.; Guizouarn, T.; Costuas, K.; Rigaut, S. *Inorg. Chem.* **2014**, *53*, 2361.
(8) Ying, J.-W.; Liu, I. P.-C.; Xi, B.; Song, Y.; Campana, C.; Zuo, J.-L.; Ren, T. *Angew. Chem., Int. Ed.* **2010**, *49*, 954. Burgun, A.; Gendron, F.; Sumby, C. J.; Roisnel, T.; Cador, O.; Costuas, K.; Halet, J.-F.; Bruce, M. I.; Lapinte, C. *Organometallics* **2014**, *33*, 2613.
(9) Anger, E.; Srebro, M.; Vanthuyne, N.; Toupet, L.; Rigaut, S.; Roussel, C.; Autschbach, J.; Crassous, J.; Réau, R. *J. Am. Chem. Soc.* **2012**, *134*, 15628.
(10) Liu, Y.; Ndiaye, C. M.; Lagrost, C.; Costuas, K.; Choua, S.; Turek, P.; Norel, L.; Rigaut, S. *Inorg. Chem.* **2014**, *53*, 8172. Li, B.; Wang, J.-Y.; Wen, H.-M.; Shi, L.-X; Chen, Z.-N. *J. Am. Chem. Soc.* **2012**, *134*, 16059.
(11) Meng, F.; Hervault, Y.-M.; Norel, L.; Costuas, K.; Van Dyck, C.; Geskin, V.; Cornil, J.; Hng, H. H.; Rigaut, S.; Chen, X. *Chem. Sci.* **2012**, *3*, 3113. Meng, F.; Hervault, Y.-M.; Shao, Q.; Hu, B.; Norel, L.; Rigaut, S.; Chen, X. *Nat. Commun.* **2014**, *5*, 3023 DOI: 10.1038/ncomms4023.
(12) Liu, K.; Wang, X.; Wang, F. *ACS Nano* **2008**, *2*, 2315. Luo, L.; Benameur, A.; Brignou, P.; Choi, S. H.; Rigaut, S.; Frisbie, C. D. *J. Phys. Chem. C* **2011**, *115*, 19955.
(13) Mahapatro, A. K.; Ying, J.; Ren, T.; Janes, D. B. *Nano Lett.* **2008**, *8*, 2131.
(14) Wen, H.-M.; Yang, Y.; Zhou, X.-S.; Liu, J.-Y.; Zhang, D.-B.; Chen, Z.-B.; Wang, J.-Y.; Che, Z.-N.; Tian, Z.-Q. *Chem. Sci.* **2013**, *4*, 2471.
(15) Lissel, F.; Schwarz, F.; Blacque, O.; Riel, H.; Lortscher, E.; Venkatesan, K.; Berke, H. *J. Am. Chem. Soc.* **2014**, *136*, 14560.
(16) Ballesteros, L. M.; Martin, S.; Marques-Gonzalez, S.; Lopez, M. C.; Higgins, S. J.; Nichols, R. J.; Low, P. J.; Cea, P. *J. Phys. Chem. C* **2015**, *119*, 784.
(17) Zhu, Y.; Clot, O.; Wolf, M. O.; Yap, G. P. A. *J. Am. Chem. Soc.* **1998**, *120*, 1812. Xu, G.-L.; Crutchley, R. J.; De Rosa, M. C.; Pan, Q.-J.; Zhang, H.-X.; Wang, X.; Ren, T. *J. Am. Chem. Soc.* **2005**, *127*, 13354. Rigaut, S.; Costuas, K.; Touchard, D.; Saillard, J.-Y.; Golhen, S.; Dixneuf, P. H. *J. Am. Chem. Soc.* **2004**, *126*, 4072. Marques-Gonzalez, S.; Parthey, M.; Yufit, D. S.; Howard, J. A. K.; Kaupp, M.; Low, P. J. *Organometallics* **2014**, *33*, 4947.
(18) Olivier, C.; Costuas, K.; Choua, S.; Maurel, V.; Turek, P.; Saillard, J.-Y.; Touchard, D.; Rigaut, S. *J. Am. Chem. Soc.* **2010**, *132*, 5638. Olivier, C.; Choua, S.; Turek, P.; Touchard, D.; Rigaut, S. *Chem. Commun.* **2007**, 3100.
(19) Vacher, A.; Benameur, A.; Ndiaye, C. M.; Touchard, D.; Rigaut, S. *Organometallics* **2009**, *28*, 6096.
(20) Field, L. D.; Magill, A. M.; Shearer, T. K.; Colbran, S. B.; Lee, S. T.; Dalgarno, S. J.; Bhadbhade, M. M. *Organometallics* **2010**, *29*, 957.
(21) Wuttke, E.; Hervault, Y.-M.; Polit, W.; Linseis, M.; Erler, P.; Rigaut, S.; Winter, R. F. *Organometallics* **2014**, *33*, 4672. Wuttke, E.; Pevny, F.; Hervault, Y.-M.; Norel, L.; Drescher, M.; Winter, R. F.; Rigaut, S. *Inorg. Chem.* **2012**, *51*, 1902. Pevny, F.; Di Piazza, E.; Norel, L.; Drescher, M.; Winter, R. F.; Rigaut, S. *Organometallics* **2010**, *29*, 5912.
(22) Grelaud, G.; Gauthier, N.; Luo, Y.; Paul, F.; Fabre, B.; Barriere, F.; Ababou-Girard, S.; Roisnel, T.; Humphrey, M. G. *J. Phys. Chem. C* **2014**, *118*, 3680.
(23) Liu, K.; Wang, X.; Wang, F. *ACS Nano* **2008**, *2*, 2315.
(24) Mahapatro, A. K.; Ying, J.; Ren, T.; Janes, D. B. *Nano Lett.* **2008**, *8*, 2131.
(25) (a) *Molecular Magnetism*; Kahn, O., Ed.; VCH: New York, 1993. (b) *Magnetism: Molecules to Materials*; Miller, J. S., Drillon, M., Eds.; Wiley-VCH: Weinheim, Germany, 2001; Vols. *I*–*V*.
(26) Paul, F.; Lapinte, C. *Unusual Structures and Physical Properties in Organometallic Chemistry*; Gielen, M., Willem, R., Wrackmeyer, B., Eds.; Wiley: New York, 2002; p 220 and references therein.
(27) Stroh, C.; Mayor, M.; von Hänisch, C.; Turek, P. *Chem. Commun.* **2004**, 2050.
(28) Ishikawa, N.; Sugita, M.; Ishikawa, T.; Koshihara, S.; Kaizu, Y. *J. Am. Chem. Soc.* **2003**, *125*, 8694. Takamatsu, S.; Ishikawa, T.; Koshihara, S.-Y.; Ishikawa, N. *Inorg. Chem.* **2007**, *46*, 7250. Ishikawa, N.; Sugita, M.; Tanaka, N.; Ishikawa, T.; Koshihara, S.-Y.; Kaizu, Y. *Inorg. Chem.* **2004**, *43*, 5498. Gonidec, M.; Davies, E. S.; McMaster, J.; Amabilino, D. B.; Veciana, J. *J. Am. Chem. Soc.* **2010**, *132*, 1756. Fortier, S.; Le Roy, J. J.; Chen, C.-H.; Vieru, V.; Murugesu, M.; Chibotaru, L. F.; Mindiola, D. J.; Caulton, K. G. *J. Am. Chem. Soc.* **2013**, *135*, 14670.
(29) Lee, J.; Lee, E.; Kim, S.; Sook Bang, G.; Shultz, D. A.; Schmidt, R. D.; Forbes, M. D. E.; Lee, H. *Angew. Chem., Int. Ed.* **2011**, *50*, 4414. Min, K. S.; Rheingold, A. L.; DiPasquale, A.; Miller, J. S. *Inorg. Chem.* **2006**, *45*, 6135. Dul, M. C.; Pardo, E.; Lescouezec, R.; Chamoreau, L.-M.; Villain, F.; Journeaux, Y.; Ruiz-Garcia, R.; Cano, J.; Julve, M.; Lloret, F.; Pasan, J.; Ruiz-Perez, C. *J. Am. Chem. Soc.* **2009**, *41*, 14614. Matsumoto, I.; Ciofini, I.; Lainé, P. P.; Teki, Y. *Chem.—Eur. J.* **2009**, *15*, 11210. Lanznaster, M.; Heeg, M. J.; Yee, G. T.; McGarvey, B. R.; Verani, C. N. *Inorg. Chem.* **2007**, *46*, 72. Newton, G. N.; Yamashita, S.; Hasumi, K.; Matsuno, J.; Yoshida, N.; Nihei, M.; Shiga, T.; Nakono, M.; Nojiri, H.; Wernsdorfer, W.; Oshio, H. *Angew. Chem., Int. Ed.* **2011**, *50*, 5716.
(30) Ito, A.; Nakano, Y.; Urabe, M.; Kato, T.; Tanaka, K. *J. Am. Chem. Soc.* **2006**, *128*, 2948.
(31) Ratera, I.; Veciana, J. *Chem. Soc. Rev.* **2012**, *41*, 303.
(32) (a) Catala, L.; Le Moigne, J.; Kyritsakas, N.; Rey, P.; Novoa, J. J.; Turek, P. *Chem.—Eur. J.* **2001**, *7*, 2466. (b) Catala, L.; Gruber, N.; Novoa, J. J.; Rabu, P.; Belorizky, E.; Le Moigne, J.; Turek, P. *Chem.—Eur. J.* **2005**, *11*, 2440.
(33) Wautelet, P.; Le Moigne, J.; Videva, V.; Turek, P. *J. Org. Chem.* **2003**, *68*, 8025.
(34) Ziessel, R.; Stroh, C.; Heise, H.; Raudaschl-Sieber, G.; Köhler, F. H.; Turek, P.; Claiser, N.; Souhassou, M.; Lecomte, C. *J. Am. Chem. Soc.* **2004**, *126*, 12604.
(35) Rajadurai, C.; Ivanova, A.; Enkelmann, V.; Baumgarten, M. *J. Org. Chem.* **2003**, *68*, 9907. Higashiguchi, K.; Matsuda, K. *Org. Lett.* **2010**, *12*, 5284.
(36) Ziessel, R.; Ulrich, G.; Lawson, R. C.; Echegoyen, L. *J. Mater. Chem.* **1999**, *9*, 1435.
(37) (a) Hicks, R. G. *Org. Biomol. Chem.* **2007**, *5*, 1321. (b) Train, C.; Norel, L.; Baumgarten, M. *Coord. Chem. Rev.* **2009**, *253*, 2342. (c) Koivisto, B. D.; Hicks, R. G. *Coord. Chem. Rev.* **2005**, *249*, 2612.
(38) (a) Takahashi, M.; Turek, P.; Nakazawa, Y.; Tamura, M.; Nozowa, K.; Shiomi, D.; Ishikawa, M.; Kinoshita, M. *Phys. Rev. Lett.* **1991**, *67*, 746. (b) Awaga, K.; Maruyama, Y. *J. Chem. Phys.* **1989**, *91*, 2743. (c) Cirujeda, J.; Mas, M.; Molins, E.; Lanfranc de Panthou, F.; Laugier, J.; Park, J.; Paulsen, C.; Rey, P.; Rovira, C.; Veciana, J. *J. Chem. Soc., Chem. Commun.* **1995**, 709. (d) Crayston, J. A.; Devine, J. N.; Walton, J. C. *Tetrahedron* **2000**, *56*, 7829.
(39) Nakano, Y.; Yagyu, T.; Hirayama, T.; Ito, A.; Tanaka, K. *Polyhedron* **2005**, *24*, 2141.
(40) Latif, I. A.; Panda, A.; Datta, S. N. *J. Phys. Chem. A* **2009**, 1595.
(41) (a) Hervault, Y.-M.; Ndiaye, C. M.; Norel, L.; Lagrost, C.; Rigaut, S. *Org. Lett.* **2012**, *14*, 4454. (b) Benameur, A.; Brignou, P.; Di Piazza, E.; Hervault, Y.-M.; Norel, L.; Rigaut, S. *New J. Chem.* **2011**, *35*, 2105.
(42) Merhi, A.; Roisnel, T.; Rigaut, S.; Train, C.; Norel, L. *CrystEngComm* **2014**, *16*, 9783.
(43) Chemistruck, V.; Chambers, D.; Brook, D. J. R. *J. Org. Chem.* **2009**, *74*, 1850.

DOI: 10.1021/acs.inorgchem.5b00667
Inorg. Chem. 2015, 54, 6347–6355

(44) Gauthier, N.; Tchouar, N.; Justaud, F.; Argouarch, G.; Cifuentes, M. P.; Toupet, L.; Touchard, D.; Halet, J.-F.; Rigaut, S.; Humphrey, M. G.; Costuas, K.; Paul, F. *Organometallics* **2009**, *28*, 2253.
(45) Marqués-González, S.; Parthey, M.; Yufit, D. S.; Howard, J. A. K.; Kaupp, M.; Low, P. J. *Organometallics* **2014**, *33*, 4947.
(46) Neugebauer, H. F. F. *Angew. Chem., Int. Ed. Engl.* **1980**, *19*, 724.
(47) Hui, P.; Arif, K. M.; Chandrasekar, R. *Org. Biomol. Chem.* **2012**, *10*, 2439.
(48) Franz, B.; Fischeri, H. *Angew. Chem., Int. Ed. Engl.* **1980**, *9*, 724.
(49) Bleaney, K. D.; Bowers, B. *Proc. R. Soc. London, Ser. A* **1952**, *214*, 451.
(50) Poddutoori, P. K.; Pilkington, M.; Alberola, A.; Polo, V.; Warren, J. E.; van der Est, A. *Inorg. Chem.* **2010**, *49*, 3516. Suzuki, S.; Yokoi, H.; Kozaki, M.; Kanzaki, Y.; Shiomi, D.; Sato, K.; Takui, T.; Okada, K. *Eur. J. Inorg. Chem.* **2014**, 4740. Stroh, C.; Turek, P.; Rabu, P.; Ziessel, R. *Inorg. Chem.* **2001**, 5334.
(51) Jurgens, O.; Vidal-Gancedo, J.; Rovira, C.; Wurst, K.; Sporer, C.; Bildstein, B.; Schottenberger, H.; Jaitner, P.; Veciana, J. *Inorg. Chem.* **1998**, *37*, 4547.
(52) Previous studies on Ru(II) acetylide complexes have shown that the EPR spectra of the delocalized monooxidized species showed an almost isotropic signal centered at $g = 2.018$; see refs 18 and 44.
(53) This agent is particularly useful for such a study because the reaction is irreversible as Au(0) is formed and it is EPR silent at low temperature. See: Segawa, H.; Machida, D.; Senshu, Y.; Nakazaki, J.; Hirakawa, K.; Wu, W. *Chem. Commun.* **2002**, 3032. Segawa, H.; Senshu, Y.; Nakazaki, J.; Susumu, K. *J. Am. Chem. Soc.* **2004**, *126*, 1354.
(54) D'Anna, J. A. *J. Chem. Phys.* **1970**, *53*, 4047.
(55) Tanaka, M.; Matsuda, K.; Itoh, T.; Iwamura, H. *J. Am. Chem. Soc.* **1998**, *120*, 7168. Maspoch, D.; Ruiz-Molina, D.; Wurst, K.; Vidal-Gancedo, J.; Rovira, C.; Veciana, J. *Dalton Trans.* **2004**, 1073.
(56) Chittipeddi, S.; Kromack, K. R.; Miller, J. S.; Epstein, A. J. *Phys. Rev. Lett.* **1987**, *58*, 2695. Beni, G.; Pincus, P.; Hone, D. *Phys. Rev. B* **1973**, *8*, 3389.
(57) Touchard, D.; Haquette, P.; Guesmi, S.; Le Pichon, L.; Daridor, A.; Toupet, L.; Dixneuf, P. H. *Organometallics* **1997**, *16*, 3640.
(58) Chaudret, B.; Commengues, G.; Poilblanc, R. *Dalton Trans.* **1984**, 1635.
(59) Ishida, T.; Iwamura, H. *J. Am. Chem. Soc.* **1991**, *113*, 4238.

DOI: 10.1021/acs.inorgchem.5b00667
Inorg. Chem. 2015, 54, 6347−6355